Luminescent carbon nanoparticles separation and purification

Alina A. Kokorina, Andrei V. Sapelkin, Gleb B. Sukhorukov, Irina Yu Goryacheva

PII: S0001-8686(19)30215-5

DOI: https://doi.org/10.1016/j.cis.2019.102043

Reference: CIS 102043

To appear in: *Advances in Colloid and Interface Science*

Revised date: 25 September 2019

Please cite this article as: A.A. Kokorina, A.V. Sapelkin, G.B. Sukhorukov, et al., Luminescent carbon nanoparticles separation and purification, *Advances in Colloid and Interface Science*(2018), https://doi.org/10.1016/j.cis.2019.102043

Luminescent carbon nanoparticles separation and purification

Alina A. Kokorina[a*], Andrei V. Sapelkin[a,b], Gleb B. Sukhorukov[a,b], Irina Yu. Goryacheva[a]

[a] Saratov State University, Astrakhanskaya Street 83, 410012 Saratov, Russia

[b] Queen Mary University of London, Mile End Road, London, E1 4NS, UK

* Corresponding author: alinaa.kokorina@gmail.com, tel. +7(951)8861027

ABSTRACT

Nowadays luminescent carbon-based nanoparticles can be synthesized by a wide range of physical and chemical methods from a large variety of carbon-based material sources. However, in most of the cases the product of synthesis is a complex mixture of compounds, which results in significant challenges in understanding the structure and optical properties of the reaction products. Consequently, a number of separation and purification methodologies have been developed to alleviate these challenges. In this review, we provide a detailed analysis of the current state of the art for methods of luminescent carbon nanoparticles separation and purification. We specifically target such methods as sucrose density gradient centrifugation, chromatography techniques, and electrophoresis because of their ability for fine separation of the reaction products with into a number of fractions. The aim of our comparative analysis is to help development of future strategies for reaction product separation and purification leading to a better understanding of carbon nanoparticles structure and luminescent mechanism as well as to underpin their applications.

CONTENT

1. Introduction

Luminescent carbon nanoparticles (CNPs) are a new class of low-dimensional nanomaterials that became very popular over the last decade since they can potentially be used as a viable alternative to the traditional semiconductor quantum dots (QDs) and have already been proposed for a number of research and technological applications. Both CNPs and QDs have several significant advantages over traditional organic fluorophores such as stable luminescence [1,2], tunable excitation and emission spectra [3–5], large surface area [6,7], resistance to photo- and chemical degradation [8] and low toxicity [9].

In this review as luminescent CNPs we understand carbon nanomaterials that have been reported in different manuscripts as carbon dots, carbon quantum dots, graphene-based nanoparticles, etc.

The common of these structures are the presence of a large number of graphene like carbon-carbon bonds with sp^2 hybrid orbitals of carbon atoms and defects areas with sp^3 carbon atoms hybridization. The well-known carbon nanostructures like carbon nanotubes, nanodiamonds or fullerenes have not been considered in this review because of the availability of a large number of articles concerned with their purification and separation techniques [10–12].

There is a large selection of starting materials and reported methods for the synthesis of CNPs. Starting materials vary from standard chemical reagents (citric acid [13], p-phenylenediamine [14], and diaminonaphthalene [15], etc.) including polymers and biopolymers (carbohydrates [16]), to laboratory-produced chemicals (surfactant-modified silica spheres [17]) or even natural products (candle soot [18], lemon peels [19], etc.). Synthesis approaches include laser ablation, electrochemical, microwave (MW) or hydrothermal (HT) treatment [20–23]. So far, none of these methods allow obtaining nanoparticles with uniform size and properties and do not provide sufficient control over CNPs' size and properties. Hence, for a detailed understanding of CNPs structure and properties as well as to enable their widespread application, it is necessary to develop

methods of separation of the reaction products with identical (or at least similar) characteristics.

Centrifugation and filtration are widely used for removing of larger fragments such as soot from CNPs suspensions. Dialysis allows addressing the problem of CNPs solution purification from smaller structures including molecules and untreated compounds. However, these methods have not delivered isolation of the CNPs with uniform properties (or even uniform size) or CNP fractions with the target properties. Methods for fine separation of CNPs mixture into more defined fractions are less described, but some very useful examples of separation into components with different properties have already been developed (examples are presented in Table 1).

Many of the approaches for separation and purification of nanoparticles described in this review are similar (or identical) to the methods of purification and fractionation developed over decades for other carbon nanostructures (generally carbon nanotubes (CNT) [10,24]). However, unlike in case of CNPs, the structure of such systems was generally known and separation methods were developed to obtain known fractions with similar properties for applications. In the case of CNPs in many cases there is a significant dispersion of the reaction products by size, defects structure, and luminescent properties. All of these features are not yet well-understood because of the difficulties of the separation of individual components from the complex mixture of the reaction products. Moreover, the exact atomic structure of CNPs is not yet known in many cases.

Thus, in this review we summarize and provide critical analysis of application of well-established separation methods (e.g. by size, mass, charge, density or, hydrophobic or hydrophilic nature) for CNPs for exploration of their properties, luminescent mechanism and potential applications. We have summarized CNPs isolation approaches together with the characteristics of separation processes and obtained compounds in Table 1. Principles and possibilities of CNPs separation techniques were summarized in Table 2.

2. Dialysis

Dialysis is a widely used technique for separation of colloidal solutions of proteins [25,26], polymers [27], and metal nanoparticles [28] from low-molecular weight substances using a semipermeable membrane. In the dialysis process, low-molecular compounds penetrate through the membrane pores (dialysate) while the high-molecular weight compounds are kept in the dialysis bag and called dialyzed solution. Usually, dialysis is used

against pure water or buffer (if it is necessary to keep pH value) for 12 - 48 hours [29–31]. While dialysis is a useful method for removal of low-molecular substances from CNPs solution, it still has a significant drawback since the dialyzed sample gets diluted. Practically, for CNP dialysis the membranes with a molecular weight cut-off (MWCO) from the smallest (100-500 Da) to 14 kDa or even more are used [31–33]. There are a large number of publications where dialysis is used as a main or one of separation method. In this part we summarize a few examples presented in order of increasing of dialysis bag pore size.

Hu's group [32] used dialysis membrane with small pores of 100-500 Da for purification HT obtained CNPs. As a result, CNPs with the average size of 5 nm with emission at 456 nm and quantum yield (QY) 38.7% were obtained. Other groups [29,34] used dialysis membranes with larger MWCO (1000 Da) for separation of hydrothermally treated solutions. The Wang et al. [34] obtained the CNPs with bright emissive at 420 nm from m-aminobenzoic acid with the QY = 30.7% and size around 3 nm. Kumar et al. [29] used dialysis process as a second separation step after filtration for nanoparticles based on Tulsi leaves with emission maxima in the area of 510-550 nm and 9.3% QY. The size of CNPs was also relatively small with an average diameter of 3 nm. The increasing of dialysis MWCO to 3500 Da leads to obtain a similar size nanoparticles around 3 nm from HT heated (2-pyridylazo)-2-naphthol and cobalt chloride. The emission maxima of CNPs are located in a green region (max 564 nm) with a QY of 6.2% [33]. Dialysis bag with larger MWCO of 8000-14000 Da was used by Mao's group [31] for separation bare CNPs and PEG-passivated ones. The reported CNPs had sizes of around 1.5 nm and emission maxima at 520-560nm; the QY was measured with different excitation wavelengths, the highest value was around 0.87% for bare CNPs and 1,24% for PEG-modified nanoparticles.

Correlation of proteins mass (in Da) with their minimum radius (in nm) allows to assume the correlation of CNPs size with dialysis bag pores [35]. Thus, the pores around 5 kDa can be passed through by nanoparticles with the sizes 1 nm or less. Hence, dialysis is usually used as one of separation methods mainly at start of treating the synthesized mixture in order to remove low molecular weight components. From the theoretical point of view, the main principle of dialysis separation is based mostly on particle size. Hence, if the particles size is larger than the pore size of a membrane, they cannot leave the dialysis bag and contribute to the substance characteristics after dialysis. Otherwise, if the substances size is smaller than the pore size, the substance proposes penetration through the dialysis membrane and leaving the bag. One of the main findings in this section is that there doesn't seem to be a clear correlation between the dialysis membrane MWCO, reported particle sizes and their PL peak

emission wavelength. This suggests that dialysis is more efficient for removing an excess of reagents or reaction products of molecular sizes.

3. Centrifugation

Centrifugation is another widely used method for particles separation. The process is based on precipitation from a solution under the centrifugal force of particles with higher density, larger mass and size. In the case of CNPs, this method is used to separate larger pieces of soot obtained in the synthesis or to separate particles with a significant difference in mass/density. The centrifugal speeds in the range of 8,000-13,000 rpm are typically used for 10-30 min [36–38]. Along with dialysis, centrifugation is usually the first step after synthesis for most of the reported protocols. One of the centrifugation advantages is the possibility of separation of CNPs both in water and in organic solvents. Another advantage of the method for CNPs separation is absence of sample dilution and even the possibility for increasing concentration. Besides, varying centrifuge speeds in a wide range can provide a route for sample separation into several fractions of different mass nanoparticles. As an example, Sahu and the colleagues [39] reported applying centrifugation for fine CNPs separation prepared from orange juice via the HT method into two fractions of distinct sizes. They used two different centrifugation speed modes: 3,000 and 10,000 rpm with interim acetone addition for successive separation of CNPs with the size of 20 nm and 1.5-4.5 nm, called CP and CD, respectively. It was found that these two fractions show different emission maxima (474 nm for CP and 455 for CD) and different QY (20% for CP and 26% for CD).

A number of reports demonstrate application of centrifugation as a method for removing of waste products such as soot or amorphous carbon. Jia and coworkers [36] synthesized CNPs from ascorbic acid and $Cu(Ac)_2 \cdot H_2O$ by HT process and used centrifugation at 8,000 rpm for separating of soot pieces. The average size of this extracted CNPs with blue-green emission in the 450-550 nm region was found to be 3.2±0.72 nm and the QY was around 3%. In another work [40] the same centrifugation speed of 8,000 rpm for 30 min was used for purification of CNPs obtained electrochemically from graphite oxide and graphite particles. The size of the obtained CNPs was 2-8 nm. The higher centrifugation speed of 10,000 rpm for 10 minutes made it possible to separate dopamine-based CNPs from larger particles [37]. After separation, the CNPs had an average size of 3.8 nm with emission maxima between 380-530 nm and a QY of 6.4 %. Similar centrifugation parameters were used by Cai's group

[41] for extracting nanoparticles with the size less than 5 nm from a solution obtained from citric acid (CA) and ethylenediamine (EDA) carbon mixture. The light emission from the CNPs were found in the blue spectral range with the maximum at 435 nm. In the recent work by Liu[38], roseheart radish based nanoparticles with the sizes of 1.2-6 nm, emission maxima at 420 nm and QY of 13.6% were obtained after high-speed centrifugation 13,000 rpm for 15 min.

In summary, centrifugation is a common method for separating a colloidal solution of carbon nanoparticles from large particles and soot pieces. No clear correlation between applied centrifugation condition, extracted particle sizes and light emission is observed. This may suggest that synthesis conditions may have significant effect of the size, structure and surface states resulting in wide variation of particle sizes.

4. Filtration

Filtration is a classical method for separation based on the substances size. A solution (or a suspension) containing different substances is passed through a material with fixed pore sizes (a filter or a membrane). CNPs with the sizes less than membrane pores can penetrate through the filter, while larger particles that cannot pass through the pores and are collected as a precipitate on the membrane surface. Limitation of this method is the absence of a possibility for obtaining fractions with a variety of sizes using single filtration.

The filtered paper with the pore size of 0.1 μm was used for separation of CNPs from non-reacted carbon tubes and graphite pieces after an oxidation process [42]. Three types of CNPs from two types of carbon nanotubes (single- and multi-walls nanotubes) and graphite exhibited similar luminescent properties with a maximum at 535 nm after filtration and dialysis. The luminescence QY of CNPs was measured to be ~3–6%; the sizes were 3-5 nm for all CNPs types.

Membranes with the pore size 0.22 μm are widely used for filtration of CNP solutions. Human hair based CNPs synthesized at three synthesis temperatures (40, 100 and 140˚C) were filtered to remove large stands of hair fibers [2]. The nanoparticles of 8.5, 4.2 and 3.1 nm sizes were obtained for different synthesis temperatures. The emission was found to be in the range of 320-450 nm for all CNPs while QYs were 11, 4 and 5.4%, respectively. The same membrane was used for the separation of three CNP types synthesized from various plant leaves[43]. Obtained CNPs had a size around 4 nm with an emission maximum at 430 nm and QY in the range of 11.8 – 16.4%. CNPs of similar size (around 4.3 nm) were obtained

after filtration of HT-treated ginger juice[44]. The emission maximum was at 420 nm with QY 13.4%. Yang's group[45] worked with a larger pore size of 1.0 μm for removing carbon substances after HT treatment of glucose and potassium dihydrophosphate. They synthesized two types of CNPs depending on starting materials ratio: C-blue (emission at 435 nm, QY 2.4%) and C-green (emission at 510 nm, QY 1.8 %) with distinct sizes of 1.83 nm and 3.83 nm respectively.

One can conclude that simple filtration does provide efficient separation of smaller particles from the larger ones, but cannot be efficiently used for tunable particle selection form the reaction solution. From the collected data it is clear that the pore diameter (0.1 – 1 μm) is much larger than the size of obtained CNPs. Therefore, it appears that the pore size does not influence the penetration of CNPs, and filtration is mostly a method for removing large size fractions. The advantages of the method are simplicity and rapidity. However, filtration is a less popular method for primary separation compared centrifugation because of a significant drawback – carbon species sticking to the filter material and blocking the pores, it can be necessary applying ultrasonication to prevent the filter blocking.

5. Sucrose Density Gradient Centrifugation

Sucrose density gradient centrifugation is a way for substances separation based on their different sedimentation in the high viscosity media. The sucrose gels with different densities (determined by the sucrose concentration) are prepared before the separation and deposited into a plastic tube as discrete layers, starting with gel with the highest sucrose concentration and so the highest density, thus providing density gradient. The sample is carefully placed on the surface of a gradient whose density increases from top to bottom. For the CNPs separation, 50-100% sucrose gel layers are typically used. Under a centrifugal force, sample penetrates into different sucrose layers. At the end, the substances form bands between the layers related to nanoparticles density.

Oza's group [46] separated CNPs ultrasonic prepared from lemon fruit into two fractions with different optical properties in 50-100% sucrose gradient. The centrifugation at 5,000 rpm for 1 hour was used. The CNPs fractions had significantly different sizes: the size of the first fraction was 20 nm and for the second it was 5 nm. The smaller size fraction (5 nm) have traveled a longer route than the larger one and stopped between the layers with higher density. In this case, the smaller CNPs from the second fraction are supposed to have a

larger density comparative to the first fraction nanoparticles. The luminescent spectra have the maxima in the region of 310-340 nm for the first fraction while for the second fraction the emission range is significantly wider: around 325-550 nm. The QYs were 12.1% and 15%, respectively.

The same sucrose gradient (50-100%) was used in the other two reports [47,48] where CNPs were prepared from Arabic gum by MW treatment. After separation, Thakur's group [47] obtained three different color fractions designated i, ii and iii (Fig. 1).

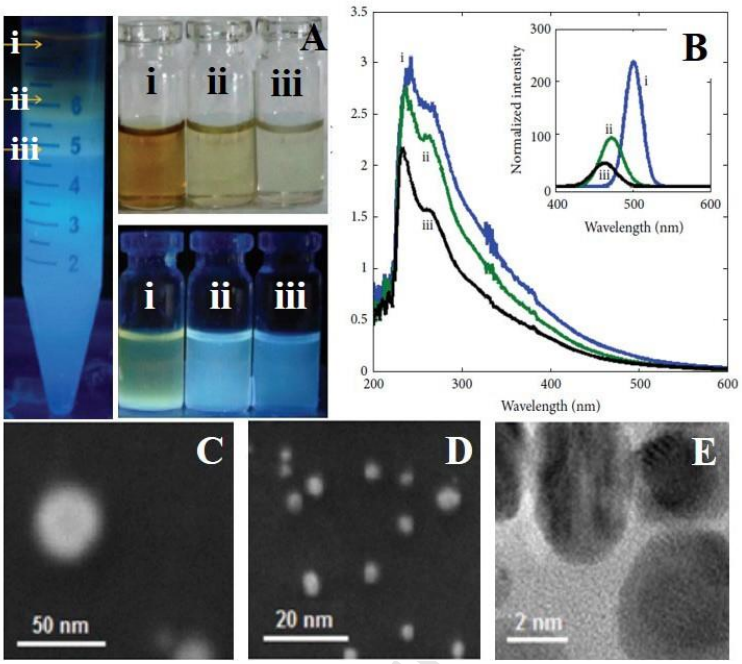

Fig. 1. Separation of CNPs using sucrose density gradient centrifugation at UV lamp (excitation 250 nm) (A, left); Upper and lower panels show the color of the fractions under normal light and UV light, respectively (A, right). Absorbance and luminescent spectra (inset) of CNPs fractions (B). SEM images (C,D) and HRTEM image (E) of fractions i, ii, and iii, respectively. Adapted with permission from Ref. [47]. Copyright (2014) Hindawi Publishing Corporation.

The luminescent maximum for fraction designated as "i" was at 500 nm, for "ii" - around 472 nm, while for "iii" it shifted down to 463 nm. Here was a similar correlation to Oza [46] results in the particle size and their way in the sucrose gradient. The smallest particles "iii" with the size around 7 nm have a longer route in the sucrose gradient and probably have the larger density comparative to fractions "ii" and "i". The middle position and the size around 10 nm was for the fraction "ii"; the biggest CNPs ("i", 30 nm) collected in the top part of the sucrose gradient with minimal density. The QYs were calculated at three different excitation

wavelengths (350, 400 and 450 nm) and all results were less than 1 %. Pandey and co-workers [48] also obtained three fractions of CNPs produced from gum Arabic extract using centrifugation with a 50-100% sucrose gradient at 2795 g for 40 min. Fraction 1 was dark brown under white light and blackish green under UV light (PL at 495 nm), the authors supposed presence of mixture graphene oxide and CNPs. In comparison to fraction 1, the absorption band of fraction 2 was at shorter wavelength area at 216 nm that can be characteristic of pure CNPs. The PL spectrum shows a maximum at 511 nm. The third fraction had a strong absorption at 215 nm and intense PL peak at 545 nm. The first fraction contains small graphene oxide sheets of 150 nm, the sizes of second and third fractions were around 5-15 nm.

The reported works show a clear correlation between the particle sizes and their position in a sucrose gradient. As can be seen, the smaller size nanoparticles collected in a layer with a larger density compare to the larger ones, which is indicated by their penetration to the sucrose layers with larger density. Hence, this method allows separating CNPs by size and particles density. Thus, being a more complex method, the density gradient centrifugation allows for a fine CNPs separation into fractions with different properties. The advantage of this method in that it offers a way for the separation of components with different density from each other. For preparative isolation of separated components, several ways can be used. One way is freezing and slicing of the sucrose layers. The other way is pricking the plastic tube to collect separated bands of substances. Sucrose density gradient centrifugation is a rarely used method due to difficulties in sucrose gradient preparation. It is also vital to avoid mixing of sucrose layers with similar densities. Finally, it is necessary to extract CNP by separation fractions from the sucrose molecules, which can be a challenge.

6. Chromatography

6.1. Size-exclusion chromatography

Size-exclusion chromatography is used for polymers [49], biopolymers [50], nanoparticles [51] separation by size due to the different ability of substances to penetrate into pores of the stationary phase. If a compound can enter the pores, it moves by a longer route than other substance with sizes larger than pores. Large substances that cannot enter the pores move through the column with the mobile phase. The smallest compounds will leave the

column the last. For separation commercial columns with size-exclusion chromatography resin as well as desalting columns are available. In standard protocol, the sample solution is placed on the top of the column and then water or buffer are added for elution of the sample fractions. The larger substances leave the column first due to exclusion from the pores of the stationary phase, while small size substances penetrate into the pores freely and leave column the last. Gravity type chromatography allows separating initial samples into a large number of fractions. The disadvantage of gravity size exclusion chromatography is dilution of substances with the water or buffer as well as long process duration. Faster separation time can be achieved by compressed gas (air, nitrogen or argon) used for pushing a mobile phase through the column. The centrifugal (spin) column chromatography provides faster separation, but there is the possibility to obtain only one fraction. This method avoids the large sample dilution and usually used for removing low molecular weight compounds (inorganic salts, for example).

A large number of scientific groups use Sephadex columns with a dextran gel of different pose size as a stationary phase. In particular, Sephadex G-100 (exclusion volume 4-150 kDa) was used by scientific teams [52,53] for separating luminescent fractions from carbon mixture. Anilcumar and colleagues [52] separated the most luminescent fraction (with QY around 78 %) after laser ablation of carbon target. The emission maximum was in the area of 550 nm for the average particle size of about 5 nm. Wang's group [53] separated candle soot-based CNPs into seven fractions. Finally, all samples have strong green emission in the area of 530 nm. The fractions QYs were significantly different, becoming progressively higher in last fractions (55-60%). The TEM data show slightly smaller particles (around 3 nm) for the most intensive luminescent seventh fraction. Kokorina and co-workers [51] used smaller exclusion volume column (1-5 kDa) Sephadex G-25 medium for fractionation of CNPs synthesized from sodium dextran sulfate. The mixture was separated into 48 fractions. The authors found three types of luminophores: the first one with emission maxima at 420 nm appears in 8-15 fractions, the second with 480 nm (10-19 fractions) and the third with 530 nm (fractions 35-48) (Fig.2). The TEM images of the fractions with the brightest emission of each type showed small CNPs sizes – from 1 to 2.3 nm. The two larger CNPs types exhibited an excitation-dependent emission, typical for CNPs. The third type of CNPs showed no-excitation-dependent emission and was the smallest in size - 1 nm. It was speculated that CNPs mixture contains molecular luminophore at latest fractions.

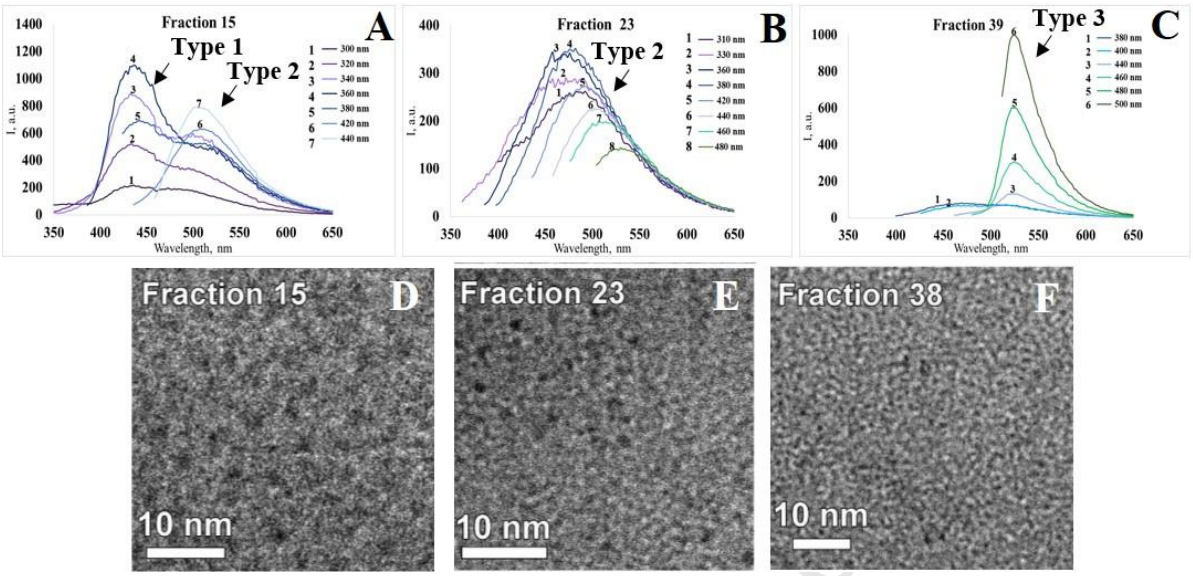

Fig. 2. Luminescent spectra of fractions with different retention volume: A- 11 ml (fraction 15); B- 16 ml (fraction 23); C- 27 ml (fraction 39). High-resolution TEM images of CNPs for fractions 15 (D), 23 (E) and 38 (F). Adapted with permission from Ref. [51]. Copyright (2017) Elsevier Ltd.

Using the Sephadex LH-20 (exclusion volume 4-5 kDa) with the pressure of 150 psi Arcudi's group [54] improved separation efficiency. CNPs were prepared from arginine and ethylenediamine. After all separation steps, three fractions with different optical properties were obtained. The first fraction had an absorption maximum at 315 nm and emission at 380 nm. The second fraction had two absorption maxima at 285 and 315 nm, the PL maximum at 357 nm. The third had two short-wave absorption maxima at 253 and 278 nm and one more long-wave at 328 nm. The sizes of CNPs were around 2.6, 2 and 1.2 nm respectively. The emission maximum for the last fraction has a red-shift compared to the first and the second fractions. The larges value of QY was measured for the smallest size fraction (19%), while for the rest of fractions QY was around 10-11%.

Wang et al. [55] worked with silica gel flash column chromatography using CH_2Cl_2/CH_3OH (10:1, v/v) as effluents. Hydrothermally prepared CNPs from *m*-aminophenol, passivated with hydrochloric and nitric acid were successfully separated into seven fractions. The emission maxima strongly red-shifted upon the increase in fraction number (450, 515, 520, 534, 550, 575, and 611 nm for fractions 1-7, respectively). The particles sizes after separation were in the range of 1.8-4.3 nm. The maximum QY was around 28%.

In conclusion, the size-exclusion chromatography provides an effective tool for extracting fractions with different properties (optical and/or size) that is essential for consequent comparative analysis. Furthermore, obtained fractions dissolved in the same buffer as CNPs start solution and there is no need for additional purification. However, it is impossible to use organic solvents in working with Sephadex columns, this method is applicable only for hydrophilic CNPs.

6.2. Anion-exchange high-performance liquid chromatography (AE-HPLC)

Ion exchange chromatography allows separating substances on the basis of ionic interactions. The stationary phase with charged functional groups interacts with the ionized substances of the opposite charge. Anion-exchange chromatography is used for separation of a negatively charged of sample of interest in the positively charged stationary phase. Thus, the sample penetrates through the column and in the case of an anion-exchange type the positive molecules will elute out first, while negatively charged molecules can be eluted by the changing of buffer pH.

The Vinci's team [56] used the chromatographic column consisting of anion-exchange polymer-based nanoparticles with 2000 Å pore size for separation of oil lamp CNPs. The elution process was accomplished by a gradient of 240-600 mM of ammonium acetate solution. These CNPs were separated into 29 fractions with different colors; the light emission maxima in the region of 380-580 nm (Fig. 3). Absorbance showed a maximum at 230 nm and a shoulder in the area around 300 nm. The average CNPs' size was 4-5 nm. The other work of this group [57] demonstrates CNPs prepared from oxidized graphene nanofibers. After separation of CNPs, 12 fractions were obtained with wide absorbance between 225-500 nm. The nanoparticles sizes had no correlation with fraction number: 10 nm for fraction 5, 7 nm for fraction 7, 14 nm for fraction 8 and 9.5 for fraction 12. There was also no correlation reported between QYs and the fraction number. The largest QYs were for the fractions 7 and 8 (7 and 6%, respectively). Fractions 5 and 10 had QYs 3 and 2%, respectively. All things considered it was found that the smallest CNPs have the longest emission at 525 nm and the largest QY (7%).

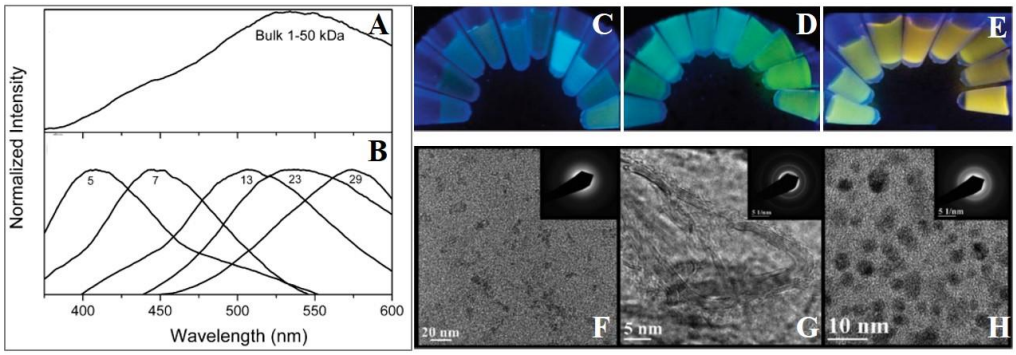

Fig. 3. Emission spectra (λ_{ex} = 325 nm) of the bulk CNPs (A) and five selected fractions (B). Photo of the fractionated species from the soot-derived sample under UV lamp (C-E). TEM images and electron diffraction patterns of particulates: fraction 3 (F), fraction 9 (G) and fraction 28 (H). Adapted with permission from Ref. [56]. Copyright (2012) American Chemical Society.

Anion-exchange chromatography provides a possibility to separate samples by the charge interaction. The difference in values of the particles surface charges allows to separate particles with different negative charge: the larger a component total negative charge, the stronger its interaction with the stationary phase and the slower it migrates into the column. Thus, the method allows separation based chiefly on the surface properties of the nanoparticles. The results obtained so far suggest the correlation between the fraction number (and so the charge of the surface of CNP) and the emission wavelength. According to the theory, first fractions have a positive or low negative charge and they show emission in a blue area, after the increasing of the CNPs negative charge (in lager fractions) the emission shifts to a green area and the most negative CNPs from the late fractions have the longest emission wavelength. These correlations may indicate that the surface charge (and so the groups determining the surface charge) make a decisive contribution to the luminescence.

.

6.3. Reversed-phase liquid chromatography and HPLC

Reversed-phase liquid chromatography is a type of liquid column chromatography with a nonpolar stationary phase and efficiency of substance separation can be controlled by the polarity of the mobile phase. As usual, C_{18}-modified silica is used as a stationary phase. The hydrophobic substances are absorbed by stationary phase and hydrophilic substances move faster through the column and elute first. The technique requires applying a mixture of

water and organic solvents; popular solvents are methanol, tetrahydrofuran, acetonitrile, ethanol, etc. This represents a significant disadvantage due to possible influence an organic solvent on a sample structure.

CNPs synthesized from urea and *p*-phenylenediamine with the 1:1 ratio by HT method were separated by reversed-phase liquid chromatography [58]. The polarity of the eluting solvents was gradually increased to obtain the fractions. Four typical fractions exhibiting blue, green, yellow, and red fluorescence were selected for further characterization Absorbance spectra had maxima at 383, 410, 488 and 528 nm for four fractions, respectively (Fig. 4). Authors explain the difference through the contribution of different surface states. The emission properties were also different for the fractions: the emission maxima at 440 nm for the first, 517 nm for the second, 566 nm for the third and 625 nm for the fourth. Obtained samples have a similar average size of around 2.6 nm and the QYs ranging from 8 to 35%.

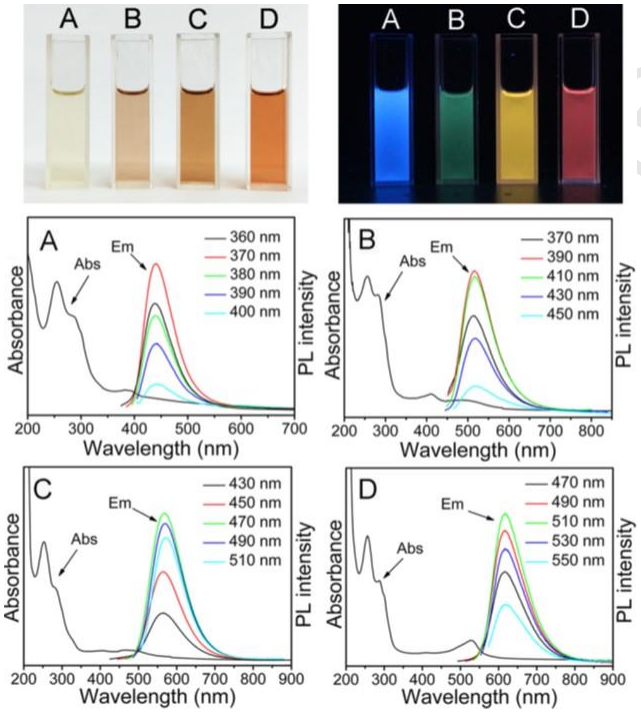

Fig. 4. Top images are photographs of samples A, B, C, and D in aqueous solution under daylight (left) and UV light (right). The bottom four graphs show their absorption curves (Abs) and their PL emission spectra (Em) under excitation with light of different wavelengths. Reprinted with permission from Ref. [58]. Copyright (2012) American Chemical Society.

A significant disadvantage of this method is a long time (about 10 hours) required for complete fractionation of CNPs reaction solution. The high-performance liquid chromatography mode (HPLC) is used to reduce time of fractionation. Methanol or its

mixture was applied as a mobile phase for CNPs separation. Gong and his team [59] used a mixture of methanol and NH_4Ac buffer as a mobile phase for separating CNPs prepared from glacial acetic acid and phosphorus oxide (V). They obtained 13 sample fractions with absorption in the range of 225-325 nm and emission in a blue-green region (450-490 nm). The sizes were analyzed for several fractions 1, 6, 8 and 12; they were 6.13 nm, 8.31 nm, 2.22 nm, and 8.66 nm, respectively. The QY data were different for these fractions with the lowest value obtained for fraction 1 (1.16%) and the maximum QY was for the fraction 4 (9%).

Gong [60] also separated CNPs prepared from chitosan and glacial acetic using this type of chromatography. The mixture of methanol and water was used as the mobile phase. As a result, 12 fractions were obtained with an absorbance peak at 300 nm and emission maxima in blue area between 400 and 415 nm. The size of CNPs increased with the increasing of fraction number: fraction 1 - 1.6 nm, fraction 3 - 1.8 nm, fraction 6 - 2.5 nm, fraction 10 - 3.1 nm.

Hu and colleagues [61] worked with RP-HPLC and used pure methanol as a mobile phase. CNPs were prepared from CA and EDA by MW synthesis and separated into 10 fractions. The absorbance maxima were detected at 240 and 334–350 nm. The latter were interpreted as corresponding to the surface trap states. The emission bands are red-shifted from 424 to 436 nm and from 442 to 450 nm for several fractions. The sizes were 1.2–3.4 nm. The maximum QYs were recorded for fractions 3, 9 and 10 (10.03%, 14.98%, and 15.83%, respectively). For the rest of the fractions, the QY was found to be below 7.0 %.

Reversed-phase liquid chromatography is a promising method due to the possibility of separating and exploring the samples mixture based on hydrophobicity, which is a surface property and allows to separate hydrophilic and hydrophobic substances. It follows from the examples that the hydrophilic CNPs (and so the smaller numbers of fractions) have a shorter emission than hydrophobic ones.

6.4. Thin-layer chromatography (TLC)

TLC is a version of chromatography for separation of samples in a thin layer of stationary phase (cellulose, silica gel or aluminum oxide). For the mobile phase, different polar or nonpolar solvents (such as ethanol, acetonitrile, dimethylformamide, water, acetone, benzene, etc.) and their mixtures can be used. A sample is placed onto the start line on the surface of the stationary phase and then proceed to move with the mobile phase. Capillary action leads to the components moving with different speed, causing sample separation into

different zones. TLC provides great opportunities for analysis and separation of substances because the method is simple and fast, while both the stationary and mobile phases can be varied. It should be noted that TLC allows washing of the separated zones for the analysis of separated fractions luminescent data and other necessary properties.

Reversed-phase TLC was used by Zhou team [62] with a C_{18}-silica stationary phase and a mixture of water and acetonitrile (7:3; v/w) as a mobile phase. The four luminescent fractions were obtained after 40 min separation of CA and EDA based CNPs (Fig. 5). The emission maxima were found to be in the range of 250-500 nm with the average CNP sizes of 3-4 nm. The QYs were different for the fractions, the largest value was for the fraction 2 (55%) and the smallest one was for the fraction 3 with 3%.

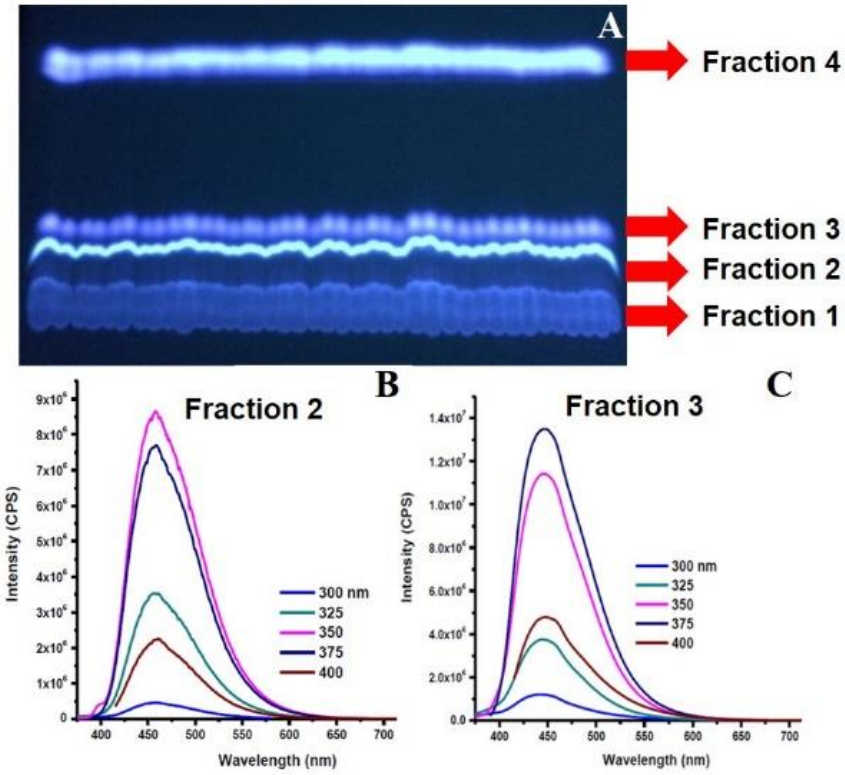

Fig. 5. CNPs fractions (1, 2, 3 and 4) on a reversed-phased TLC plate (A); Luminescent spectra of the CNPs fractions 2 (B) and 3 (C). Adapted with permission from Ref [62]. Copyright (2012) ChemPub Society.

A large variety of commercially available TLC plates and a wide range of mobile phases make this method promising for application in a nanoscale area. However, the necessity to elute separated CNPs fractions and technical difficulties of elution closely-spaced sample fractions can reduce the popularity of this method.

7. Electrophoresis

7.1. *Gel electrophoresis*

Electrophoresis is a technique for separation of charged substances in a conductive media in the electric field. Application of viscous media, such as gel slows migration speed and makes it dependent on the substances size and charge. Gel electrophoresis is thus a method of separation by charge-to-size ratio in the electric field in a viscous media, formed using different gel types and concentrations. In addition, this method allows discriminating by positive or negative charge of the separated substances.

For separation of carbon-based nanostructures gel electrophoresis, first time was used by Xu's team [63] in 2004 for purifying of single-walled carbon nanotubes. They worked with 1% agarose gel for isolation of nanotubes fractions and found a luminescent mixture of green-blue, yellow and orange substances; they called them fluorescent carbon. TEM images showed the average size of around 1 nm. So it is possible to suggest that it was gel electrophoresis, which introduced CNPs into scientific society.

Agarose gel with a concentration of 0.2% was used for separation CA-EDA CNPs prepared at the different synthesis time [64]. After separation, the gel lane was divided into nine areas: four with a positive and four with a negative charge, and one corresponding to the loading wells. All bands showed absorption at 350 nm and emission at around 450 nm. The sizes were similar for all species (less than 2 nm). Species with maximum negative and positive charge had stronger PL compared to other bands. Authors concluded that in the reaction small polycyclic aromatic hydrocarbons and molecules of organic fluorophore can form that can be embedded into the hydrocarbons matrix. Kokorina and co-workers [65] used agarose gel with higher concentration of 2% for CA-EDA CNPs mixture separation. They obtained four luminescent bands consisting of both positively and negatively charged species, extracted separate luminescent bands from the gel for the detailed investigation (Fig. 6). It was found that all bands have emission that originates from the fluorophore with the maximum at 450 nm. The authors confirmed presence of negatively-charged blue-emissive molecular fluorophore with the largest charge-to-size ratio and that this fluorophore shows no excitation-dependent light emission properties. The other bands contain the molecular fluorophore and the carbon species. The QYs were different for all bands: the highest one was for the «pure» fluorophore with no excitation dependence of PL (80±4 %, band 4), the band 1 has QY around 59±3 % and the lowest QYs were 33±5 % and 32±6 %, respectively for bands

2-3 (Fig. 6). Authors speculated the lower QYs values for "heavier" bands could be a result of internal filter effect due to carbon matrix presence.

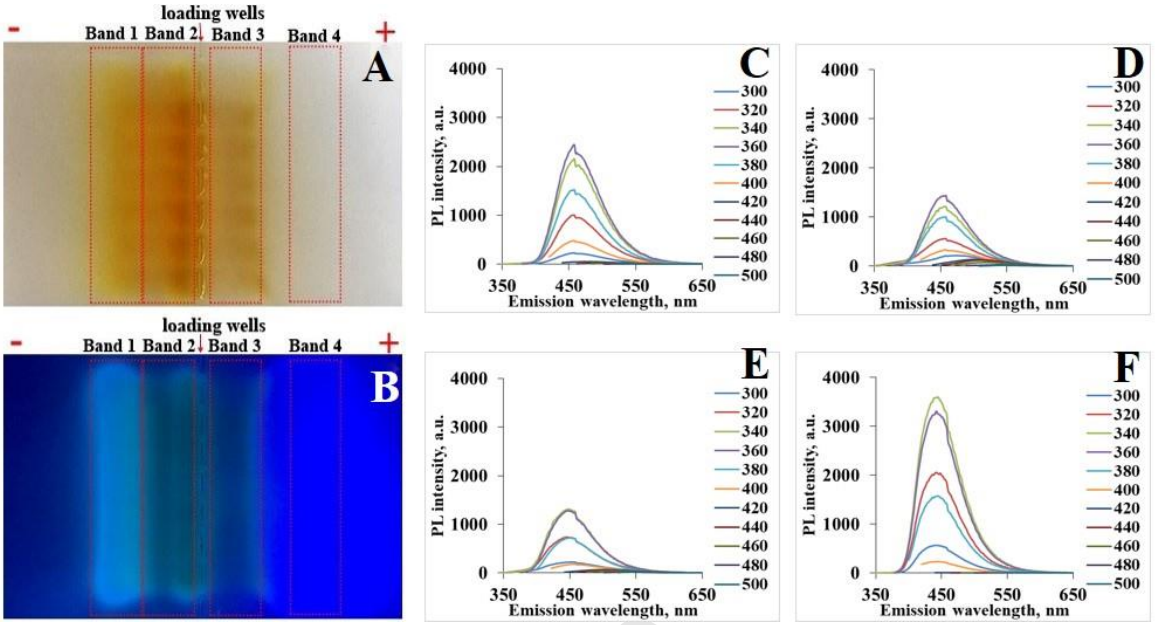

Fig. 6. Gel electrophoresis separation of CA and EDA CNPs at white light (A) and UV-light (B) photos. Luminescent spectra of extracted bands 1 (C), 2(D), 3(E) and 4(F). Reprinted with permission from Ref. [65]. Copyright 2019 Nature Publishing Group.

Liu's group [8] used another type of gel - the polyacrylamide gel - for analysis of candle soot CNPs with oxidation by nitric acid. All of the obtained bands had a negative charge. The authors classified the bands for three distinct species: nine fast-moving fluorescent bands, slow-moving, non-luminescent bands and agglomerates that did not penetrate the gel. The emission peaks for all fast-moving bands were at a region 415-615 nm. The sizes were around 1 nm and QYs were less than 1%.

Gel electrophoresis is a technique for sample separation based on charge, size and mass properties. One of the advantage is a possibility to extract sample fractions from the matrix for subsequent analysis. The selection of gel electrophoresis experimental parameters such as buffer solution, pH, amperage, gel nature, and concentration allows effective sample separation. Furthermore, the possibility of a combination of gel electrophoresis and optical detections methods can provide detailed information about the nature and origin of light emission in CNPs.

7.2. *Capillary electrophoresis*

Capillary electrophoresis is a technique based on the separation of substances by charge-to-size principle in the capillaries with the submillimeter diameter under the constant electric field. Detection of separated molecules can be provided by absorption or fluorescent detectors avoided additional purification steps.

Hu and his team [66] used capillary electrophoresis for separating neutral, positively and negatively charged species from the CA-EDA based CNPs. All fractions (ten) have absorption maxima at 250 and 350 nm. The emission maximum was in a green region at 550 nm. Reportedly, positively charged and neutral CNPs showed strongest emission while negatively charged CNPs had lower PL quantum yield.

Capillary electrophoresis can be a promising method for effective separation of complex CNPs mixtures due to several advantages like a possibility to separate ionic, neutral, hydrophilic, hydrophobic or chiral components, using a minimal volume of samples (a few microliters) and solvents and the absence of expensive columns with sorbents. Dielectrophoresis can be proposed as an extended version of capillary electrophoresis. This method allows separating substances mixture in a submillimeter capillary by alternating-electric field affecting. This technique is used for CNTs' separation by different length, diameter, a quantity of carbon layers and purification from metal particles due to their different ability of interaction with the electric field [67]. The main advantage of this method is the possibility to change the parameters of an electric field for separation of different types of CNPs and collecting them in different areas of microelectrode depending on their reaction on the alternating-electric field.

8. Concluding remarks

CNPs are a relatively new and rapidly developing class of luminescent carbon nanomaterials. Growing interest to CNPs can be correlated with a large variety of relatively cheap starting materials, a range of chemical and physical approaches, and prospective applications. For a long period, research related to CNPs was aimed at their synthesis and modification, however, a huge number of precursors and variety of synthetic conditions complicated the task of understanding the structure and luminescence mechanisms. Other difficulties were related to difficulties to control the size and structure of nanoparticles during the synthesis process. The obtained CNPs can be different in a substantially range of properties such as atomic composition and structure, density, mass, surface charge, and

hydrophobicity, light absorption and emission. Therefore, currently, one of the most challenging tasks is finding approaches for the separation of the CNPs mixture into individual components, or in as few fractions as possible, for subsequent analysis of their properties.

Commonly used centrifugation, dialysis or filtration techniques are necessary for removing large soot pieces or low molecular weight substances. An addition of techniques for fine separation (sucrose density centrifugation, gel electrophoresis, chromatography) is based on various CNPs properties, such as density, properties (charge, hydrophobicity) will allow not only to isolate CNPs fraction with uniform properties but charge, mass, size, hydrophobic or hydrophilic nature (Table 2). A step-by-step thoughtful combination of separation methods based on the size/mass/density of CNPs with following separation based on the surface properties will allow to establish CNPs' morphological characteristics, responsible for different emissive phenomena. Thus, separation approaches in combination with modern methods of the structure and luminescent properties characterization can help in formulating a unified theory for describing the CNPs structure and properties.

9. Challenges

Obviously, it has been made considerable progress in the luminescent CNPs' separation techniques for resent years. Many research groups are disquieted by necessarily of finding and optimizing the separation methods to CNPs. There are some challenges to be solved such as reproducibility, scaling-up and a combination of several methods for separation of CNPs by different properties (for example, size and hydrophobicity or charge and density). It is important to note the necessity of enhancement of synthetic approaches and using high purity chemical reagents to avoid minor products. Exact separation of luminescent CNPs' mixture by different properties fractions will lead to targeting application in medical, biological, analytical or technical areas.

Table 1. Methods of CNPs separation

CNPs start material	Synthetic method/ conditions	Separation conditions	CNPs absorbance (ABS), excitation (EX) and emission (EM) maxima, nm	Size, nm	QY, %	Reference
Dialysis						
Ethanol, H_2O_2	HT/ 180˚C, 12 h	MWCO = 100-500 Da	ABS: 222, 281, 406; EX: 400;	~ 5	38.7	[32]

			EM: 456			
M-aminobenzoic acid	HT/ 180˚C, 12 h	MWCO = 1000 Da	ABS: 300, 407; EX: 300; EM: 420	~ 3	30.7	[34]
Tulsi leaves	HT/ 180˚C, 4 h	MWCO = 1000 Da, 12 h	ABS: 280, 330; EX: 450-530; EM: 510-550	~3	9.3	[29]
1-(2-Pyridylazo)-2-naphthol, cobalt chloride	HT/ 180˚C, 4 h	MWCO = 3500 Da, against ethanol	ABS: 400-550; EX: 485; EM: 564	~2.97	6.2	[33]
Black lamp soot	HT/ 140˚C, 12 h	MWCO = 8000-14000 Da	EX: 420-500; EM: 520-560	~1.5	max: 0.87 ± 0.04	[31]
Centrifugation						
Orange juice	HT/ 120˚C, 2.5 h	Two types: (1) -3000 rpm, (2) -10000 rpm	ABS: 288; (1) EM: 474; (2) EM: 455	(1) > 20, (2) 1.5-4.5	(1) 20, (2) 26	[39]
Ascorbic acid and $Cu(Ac)_2*H_2O$	HT/ 90˚C, 5 h	8000 rpm	ABS: 287; EX: 365; EM: 450-550	3.2±0.72	3.22	[36]
Graphite rods	Electrolysis/ 15 min, 3 times	8000 rpm, 30 min	N/A	2.8	N/A	[40]
Dopamine	HT/ 180˚C, 6 h	10000 rpm, 10 min	EM: 380-530	3.8	6.4	[37]
CA, EDA	HT/ 300˚C, 5h	10000 rpm, 10 min	ABS: 340; EX: 360; EM: 435	< 5 nm	N/A	[41]
Rose-heart radish	HT/180˚C, 3h	13000 rpm, 15 min	ABS: 281.5; EX: 320; EM: 420	1.2-6	13.6	[38]
Filtration						
Carbon nanotubes (single-, multi-walled) and graphite	Sulfuric-nitric acid oxidation	Pore size 0.1 μm	ABS: 200-600; EX: 460; EM: 535	~ 3-5	3-6	[42]
Human hair	(1) HT/ 40 ˚C, 24 h (2) HT/ 100 ˚C, 24 h (3) HT/ 140 ˚C, 24 h	Pore size 0.22 μm	Three CNPs types: (1) ABS: 323; EX: 330; EM: 383; (2) ABS: 300; EX: 353; EM: 450; (3) ABS: 295; EX: 369; EM: 370	(1) 8.5, (2) 4.2, (3) 3.1	(1) 11.1, (2) 4.02, (3) 5.38	[2]
Plant leaves	Pyrolysis/ 250, 300, 350, 400˚C, 2 h	Pore size 0.22 μm	Three CNPs types depend on start material: ABS: 300; EX: 370; (ori) EM: 429; (lot) EM: 424;	~3.7	(ori) 16.4, (lot) 15.3, (pin) 11.8	[43]

			(pin) EM: 427			
Ginger juice	HT/ 300˚C, 2 h	Pore size 0.22 μm	ABS: 270, 325; EX: 325; EM: 420	4.3 ± 0.8	13.4	[44]
Glucose/KH_2PO_4 (1) – 1/36 (2) – 1/26	HT/ 200˚C, 12 h	Pore size 1.0 μm	(1-2) ABS: 250-600; (1) EX: 350; EM: 435; (2) EX: 440; EM: 510	(1) ~1.83, (2) ~3.83	(1) 2.4, (2) 1.8	[45]
Sucrose density gradient centrifugation						
Citrus lemon	Ultrasonication/ 20 kHz, 1 h	(1) 5000 rpm, 1 h; (2) 12000, 15 min 50–100% gradient concentration of sucrose	(1) ABS: 250, 350; EM: 310-340; (2) ABS: 244, 293; EM: 325-550	(1) 20, (2) 5	(1) 12.1, (2) 15	[46]
Gum Arabic	MW pyrolysis, 5 min	50–100% gradient concentration of sucrose	(1) ABS:243, 267; EM: 500; (2) ABS: 235, 265; EM: 472; (3) ABS: 232, 263; EM: 463	(1) 30, (2) 10, (3) 7	(1) 90, (2) 80, (3) 60	[47]
Gum Arabic	MW pyrolysis, 5 min	50–100% gradient concentration of sucrose, 2795 g, 40 min	Free fractions: (1) ABS: 424 and background 600; EM: 495 (2) ABS: 216; EM: 511; (3) ABS: 215; EM: 545	(2) 5-15, (3) 5-10	N/A	[48]
Exclusion column chromatography						
Carbon target, passivation with PEG_{1500N}, ZnS and ZnO	Laser ablation	Sephadex G-100	ABS: 440; EM: 520	~ 5	78	[52]
Carbon soot, PEG_{1500N} passivation	HT/ 12 h	Sephadex G-100	EM: shoulder in a blue region and 530	3	55-60	[53]
Sodium dextran sulfate	HT/ 220˚C, 3 h	Sephadex G-25 medium	48 fractions with 3 CNPs types: (1) EM: 420; (2) EM: 480; (3) EM: 530	~1-2.3	---	[51]
Arginine, EDA	MW pyrolysis/ 240˚C, 200W, 26 bar, 3 h	Sephadex LH-20 at pressure 150 psi	Three fractions: (1) ABS: 315; EM: 380; (2) ABS: 285, 315; EM: 357;	(1) 2.65±0.48, (2) 2.04±0.5	(1) 19, (2) 10, (3) 11	[54]

			(3) ABS: 253, 278, 328; EM: 421	7, (3) 1.24±0.43		
m-Aminophenol in EtOH, hydrochloric acid and nitric acid	HT/ 180˚C, 12h	Flash with using CH_2Cl_2/CH_3OH (10:1, v/v) as eluents, silica as a stationary phase	Seven fractions: (1) EM: 450; (2) EM: 515; (3) EM: 520; (4) EM: 534; (5) EM: 550; (6) EM: 575; (7) EM: 611	1.8-4.3	(2) 27.7, (3) 28.6	[55]
Anion-exchange high-performance liquid chromatography						
Oil lamp soot	Oxidation	Dionex IonPac AS12A column	29 fractions: ABS: 230, features at ~300; EM: 380-580	~ 4-5	N/A	[56]
Graphite nanofibers	Oxidation	N/A	12 fractions, analyzed 5, 7, 8, 10 ABS: 225-500; (5) EM: 450; (7) EM: 525; (8) EM: 500	(5) 10.1 ± 0.8, (7) 7.1 ± 0.6, (8) 14 ± 1, (10) 9.4 ± 0.5	(5) 2, (7) 6, (8) 7, (10) 3	[57]
Reversed-phase liquid chromatography						
Urea and p-phenylenediamine 1:1	HT/ 160˚C, 10 h	Stationary phase: silica; mobile phase: ethyl acetate and ethanol	Four fractions: (1) ABS: 200-350, 383; (2) ABS: 200-350, 410; (3) ABS: 200-350, 488; (4) ABS: 200-350, 528; (1-4) EM: 440-652	2.6	8-35	[58]
Reversed-phase high-performance liquid chromatography (C_{18})						
Glacial acetic acid, water and P_2O_5	Baking	mobile phase: MeOH and NH_4Ac buffer (pH 5.5)	13 fractions: (1-13) ABS: 225-325; (1-13) EM: 449-490	(1) 6.13, (6) 8.31, (8) 2.22, (12) 8.66	(1) 1.16, (6) 2.13, (8) 5.38, (12) 4.37	[59]
Chitosan, glacial acetic	HT/ 180˚C, 12 h	Mobile phase: MeOH and water	12 fractions: (1-12) ABS: 300; (1-12) EM: 400-415	(1) 1.6, (3) 1.8, (6) 2.5, (10) 3.1	N/A	[60]

CA, EDA	MW pyrolysis	Mobile phase: MeOH	10 fractions: (1-10) ABS: 240 and 334-350; (1-10) EX: 310-400; (1-10) EM: 430-452	1.2-3.4	(3) 10.03, (9) 14.98, (10) 15.83, other <7.0	[61]
Thin-layer chromatography						
CA, EDA	Oil bath, 160˚C, 50 min	Stationary phase: silica C_{18} gel plate; mobile phase: water: acetonitrile (7:3; v/w)	Four fractions: (1) ABS: 262, 342; EM: 425-460; (2-4) ABS: 243, 262; (2) EM: 465; (3) EM: 445; (4) EM: 425-500	(1) 4.2±1.6, (2) 2.4±0.6, (3) 3.2±0.6, (4) 3.8±0.8	(1) 4, (2) 55, (3) 3, (4) 12	[62]
Gel electrophoresis						
Carbon nanotubes	Arc-discharge	1% agarose gel	The mixture of green-blue, yellow, orange CNPs	~ 1	1.6	[63]
CA, EDA	HT/ 200˚C, 0.25, 0.5, 1, 3, 5, 10 h	0.2% agarose gel, 150V, 40 min	Nine bands: ABS: 350; EX: 350; EM: 450	< 2	N/A	[64]
CA, EDA	HT/ 200˚C, 3 h	2% agarose gel, 150V, 300 mA for 30 min	Four bands: ABS: 242, 358; EX: 350; EM: 450	N/A	(1) 59±3, (2) 33±5, (3) 32±6, (4) 80±4	[65]
Candle soot	Oxidation	polyacrylamide gel	Three classes of species: EM: 415-615	~ 1	(1) 0.008, (4) 0.019, (7) 0.008	[8]
Capillary electrophoresis						
CA, EDA	MW pyrolysis/ 4 min	N/A	Neutral, positively and negatively charged fractions ABS: 360	N/A	Positive and neutral have high QY, negative – low QY	[66]

*__Table abbreviations list:__

ABS – maxima or a range of absorbance spectra
CA – citric acid
CNPs – carbon nanoparticles

EDA – ethylenediamine
EM – maxima or a range of PL
EX – maxima of excitation spectra
HT – hydrothermal CNPs synthesis
Lot – lotus leaves
MW – microwave CNPs synthesis
MWCO - molecular weight cut-off for dialysis bag
N/A – no available data
Ori – oriental plane leaves
Pin – pine needles

Table 2. Principles and feasibilities of CNPs separation techniques

	Parameter of separation	Separation technique	CNPs properties correlation with separation parameters	Separation type	Equipment	Extraction from the matrix	Comment
1	Size	Filtration	N/A*	primary separation	filters/ membranes	-**	-
		Dialysis			membrane bags	-	minor sample dilution
		Size-exclusion chromatography		fine-separation	size-exclusion column	-	high sample dilution
2	Mass and/or density	Centrifugation		primary separation	centrifuge	-	possibility for pre-concentration
		Sucrose-density gradient centrifugation	CNPs size decrease with increasing of gradient density	fine-separation	ultracentrifuge	+***	-
3	Charge to size ratio	Gel and capillary electrophoresis	Positive-negative charge discrimination; compounds with higher charge/mass move faster		electrophoresis system, gel layer/ bare fused-silica capillary	+/- (for gel and capillary electrophoresis respectively)	-
4	Hydrophobicity	Reversed phase liquid chromatography (column)	The hydrophobic substances are absorbed by stationary phase, hydrophilic substances move		silica gel C_{18}	-	-
		Reversed phase liquid chromatography (thin-layer)				+	-

5	Charge	Anion-exchange chromatography (column)	Positively charged substances move faster, negatively charged substances can be eluted by the changing of buffer pH		chromatography system, anion-exchange column	-	-

* N/A – no available correlations or direct data comparison is impossible

** - extraction from the matrix is not necessary

*** + extraction from the matrix is necessary

Acknowledgements

The work was supported by Russian Science foundation (project 16-13-10195).

References

[1] Xu M, Gao Z, Zhou Q, Lin Y, Lu M, Tang D. Terbium ion-coordinated carbon dots for fluorescent aptasensing of adenosine 5'-triphosphate with unmodified gold nanoparticles. Biosens Bioelectron 2016;86:978–84.

[2] Sun D, Ban R, Zhang PH, Wu GH, Zhang JR, Zhu JJ. Hair fiber as a precursor for synthesizing of sulfur- and nitrogen-co-doped carbon dots with tunable luminescence properties. Carbon N Y 2013;64:424–34. doi:10.1016/j.carbon.2013.07.095.

[3] Miao X, Qu D, Yang D, Nie B, Zhao Y, Fan H. Synthesis of Carbon Dots with Multiple Color Emission by Controlled Graphitization and Surface Functionalization 2017;1704740:1–8. doi:10.1002/adma.201704740.

[4] Lv S, Li Y, Zhang K, Lin Z, Tang D. Carbon Dots / g-C3N4 Nanoheterostructures-Based Signal- Generation Tags for Photoelectrochemical Immunoassay of Cancer Biomarkers Coupling with Copper Nanoclusters Carbon Dots / g-C 3 N 4 Nanoheterostructures-Based Signal-Generation Tags for Photoelectrochemical Immunoassay of Cancer Biomarkers Coupling with Copper Nanoclusters 2017. doi:10.1021/acsami.7b13272.

[5] Feng T, Zeng Q, Lu S, Yan X, Liu J, Tao S, et al. Color-Tunable Carbon Dots Possessing Solid-State Emission for Full-Color Light-Emitting Diodes Applications Color-Tunable Carbon Dots Possessing Solid-State Emission for Full-Color Light-Emitting Diodes Applications 2017. doi:10.1021/acsphotonics.7b01010.

[6] Ming H, Ma Z, Liu Y, Pan K, Yu H, Wang F, et al. Large scale electrochemical synthesis of high quality carbon nanodots and their photocatalytic property. Dalt Trans 2012;41:9526. doi:10.1039/c2dt30985h.

[7] Hou Y, Lu Q, Deng J, Li H, Zhang Y. One-pot electrochemical synthesis of functionalized fluorescent carbon dots and their selective sensing for mercury ion. Anal Chim Acta 2015;866:69–74. doi:10.1016/j.aca.2015.01.039.

[8] Liu H, Ye T, Mao C. Fluorescent carbon nanoparticles derived from candle soot. Angew Chemie - Int Ed 2007;46:6473–5. doi:10.1002/anie.200701271.

[9] Esteves da Silva JCG, Gonçalves HMR. Analytical and bioanalytical applications of carbon dots. TrAC - Trends Anal Chem 2011;30:1327–36. doi:10.1016/j.trac.2011.04.009.

[10] Hou P, Liu C, Cheng H. Purification of carbon nanotubes 2013;6. doi:10.1016/j.carbon.2008.09.009.

[11] Yang S. Synthesis , Separation , and Molecular Structures of Endohedral Fullerenes 2012:1079–94.

[12] Zhao L, Takimoto T, Ito M, Kitagawa N, Kimura T, Komatsu N. Zuschriften Chromatographic Separation of Highly Soluble Diamond Nanoparticles Prepared by Polyglycerol Grafting 2011;4:1424–8. doi:10.1002/ange.201006310.

[13] Song Y, Zhu S, Zhang S, Fu Y, Wang L, Zhao X, et al. Investigation from chemical structure to photoluminescent mechanism: A type of carbon dots from the pyrolysis of citric acid and an amine. J Mater Chem C 2015;3:5976–84. doi:10.1039/c5tc00813a.

[14] Chen J, Wei JS, Zhang P, Niu XQ, Zhao W, Zhu ZY, et al. Red-Emissive Carbon Dots for Fingerprints Detection by Spray Method: Coffee Ring Effect and Unquenched Fluorescence in Drying Process. ACS Appl Mater Interfaces 2017;9:18429–33. doi:10.1021/acsami.7b03917.

[15] Yuan F, Wang Z, Li X, Li Y, Tan Z, Fan L, et al. Bright Multicolor Bandgap Fluorescent Carbon Quantum Dots for Electroluminescent Light-Emitting Diodes. Adv Mater 2017;29:1604436. doi:10.1002/adma.201604436.

[16] Peng H, Travas-Sejdic J. Simple Aqueous Solution Route to Luminescent Carbogenic Dots from Carbohydrates. Chem Mater 2009;21:5563–5. doi:10.1021/cm901593y.

[17] Liu R, Wu D, Liu S, Koynov K, Knoll W, Li Q. An aqueous route to multicolor photoluminescent carbon dots using silica spheres as carriers. Angew Chemie - Int Ed 2009;48:4598–601. doi:10.1002/anie.200900652.

[18] Ray SC, Saha A, Jana NR, Sarkar R. Fluorescent Carbon Nanoparticles : Synthesis , Characterization , and Bioimaging Application. J Phys Chem C 2009:18546–51.

[19] Tyagi A, Tripathi KM, Singh N, Choudhary S, Gupta RK. Green synthesis of carbon quantum dots from lemon peel waste: Applications in sensing and photocatalysis. RSC Adv 2016;6:72423–32. doi:10.1039/c6ra10488f.

[20] Baker SN, Baker GA. Luminescent carbon nanodots: Emergent nanolights. Angew Chemie - Int Ed 2010;49:6726–44. doi:10.1002/anie.200906623.

[21] Lim SY, Shen W, Gao Z. Carbon quantum dots and their applications. Chem Soc Rev 2015;44:362–81. doi:10.1039/c4cs00269e.

[22] Zuo P, Lu X, Sun Z, Guo Y, He H. A review on syntheses, properties, characterization and bioanalytical applications of fluorescent carbon dots. Microchim Acta 2016;183:519–42. doi:10.1007/s00604-015-1705-3.

[23] Kokorina AA, Prikhozhdenko ES, Sukhorukov GB, Sapelkin A V, Goryacheva IY. Luminescent carbon nanoparticles: synthesis, methods of investigation, applications. Russ Chem Rev 2017;86:1157–71. doi:10.1070/RCR4751.

[24] Li P, Kumar A, Ma J, Kuang Y, Luo L, Sun X. Density gradient ultracentrifugation for colloidal nanostructures separation and investigation. Sci Bull 2018. doi:10.1016/j.scib.2018.04.014.

[25] Reynolds JA, Tanford C. Binding of dodecyl sulfate to proteins at high binding ratios. Possible implications for the state of proteins in biological membranes. Proc Natl Acad Sci U S A 1970;66:1002–7.

[26] Kochansky CJ, McMasters DR, Lu P, Koeplinger KA, Kerr HH, Shou M, et al. Impact of pH on plasma protein binding in equilibrium dialysis. Mol Pharm 2008;5:438–48. doi:10.1021/mp800004s.

[27] Hornig S, Heinze T, Becer CR, Schubert US. Synthetic polymeric nanoparticles by nanoprecipitation. J Mater Chem 2009;19:3838–40. doi:10.1039/b906556n.

[28] Mandal D, Bolander ME, Mukhopadhyay D, Sarkar G, Mukherjee P. The use of microorganisms for the formation of metal nanoparticles and their application. Appl Microbiol Biotechnol 2006;69:485–92. doi:10.1007/s00253-005-0179-3.

[29] Kumar A, Chowdhuri AR, Laha D, Mahto TK, Karmakar P, Sahu SK. Green synthesis of carbon dots from Ocimum sanctum for effective fluorescent sensing of Pb2+ions and live cell imaging. Sensors Actuators, B Chem 2017;242:679–86. doi:10.1016/j.snb.2016.11.109.

[30] Liu J, Lu S, Tang Q, Zhang K, Yu W, Sun H, et al. One-step hydrothermal synthesis of photoluminescent carbon nanodots with selective antibacterial activity against Porphyromonas gingivalis. Nanoscale 2017;9:7135–42. doi:10.1039/c7nr02128c.

[31] Mao XJ, Zheng HZ, Long YJ, Du J, Hao JY, Wang LL, et al. Study on the fluorescence characteristics of carbon dots. Spectrochim Acta - Part A Mol Biomol Spectrosc 2010;75:553–7. doi:10.1016/j.saa.2009.11.015.

[32] Hu Y, Yang J, Jia L, Yu JS. Ethanol in aqueous hydrogen peroxide solution: Hydrothermal synthesis of highly photoluminescent carbon dots as multifunctional nanosensors. Carbon N Y 2015;93:999–1007. doi:10.1016/j.carbon.2015.06.018.

[33] Zhang HY, Wang Y, Xiao S, Wang H, Wang JH, Feng L. Rapid detection of Cr(VI) ions based on cobalt(II)-doped carbon dots. Biosens Bioelectron 2017;87:46–52. doi:10.1016/j.bios.2016.08.010.

[34] Wang R, Wang X, Sun Y. One-step synthesis of self-doped carbon dots with highly

photoluminescence as multifunctional biosensors for detection of iron ions and pH. Sensors Actuators, B Chem 2017;241:73–9. doi:10.1016/j.snb.2016.10.043.

[35] Erickson HP. Size and Shape of Protein Molecules at the Nanometer Level Determined by Sedimentation , Gel Filtration , and Electron Microscopy n.d.;11:32–51. doi:10.1007/s12575-009-9008-x.

[36] Jia X, Li J, Wang E. One-pot green synthesis of optically pH-sensitive carbon dots with upconversion luminescence. Nanoscale 2012;4:5572–5. doi:10.1039/c2nr31319g.

[37] Qu K, Wang J, Ren J, Qu X. Carbon dots prepared by hydrothermal treatment of dopamine as an effective fluorescent sensing platform for the label-free detection of iron(III) ions and dopamine. Chem - A Eur J 2013;19:7243–9. doi:10.1002/chem.201300042.

[38] Liu W, Diao H, Chang H, Wang H, Li T, Wei W. Green synthesis of carbon dots from rose-heart radish and application for Fe3+detection and cell imaging. Sensors Actuators, B Chem 2017;241:190–8. doi:10.1016/j.snb.2016.10.068.

[39] Sahu S, Behera B, Maiti TK, Mohapatra S. Simple one-step synthesis of highly luminescent carbon dots from orange juice: Application as excellent bio-imaging agents. Chem Commun 2012;48:8835–7. doi:10.1039/c2cc33796g.

[40] Zhu C, Liu C, Zhou Y, Fu Y, Guo S, Li H, et al. Carbon dots enhance the stability of CdS for visible-light-driven overall water splitting. Appl Catal B Environ 2017;216:114–21. doi:10.1016/j.apcatb.2017.05.049.

[41] Cai QY, Li J, Ge J, Zhang L, Hu YL, Li ZH, et al. A rapid fluorescence "switch-on" assay for glutathione detection by using carbon dots-MnO<inf>2</inf> nanocomposites. Biosens Bioelectron 2015;72:31–6. doi:10.1016/j.bios.2015.04.077.

[42] Tao H, Yang K, Ma Z, Wan J, Zhang Y, Kang Z, et al. In vivo NIR fluorescence imaging, biodistribution, and toxicology of photoluminescent carbon dots produced from carbon nanotubes and graphite. Small 2012;8:281–90. doi:10.1002/smll.201101706.

[43] Zhu L, Yin Y, Wang CF, Chen S. Plant leaf-derived fluorescent carbon dots for sensing, patterning and coding. J Mater Chem C 2013;1:4925–32. doi:10.1039/c3tc30701h.

[44] Li CL, Ou CM, Huang CC, Wu WC, Chen YP, Lin TE, et al. Carbon dots prepared from ginger exhibiting efficient inhibition of human hepatocellular carcinoma cells. J Mater Chem B 2014;2:4564–71. doi:10.1039/c4tb00216d.

[45] Yang ZC, Wang M, Yong AM, Wong SY, Zhang XH, Tan H, et al. Intrinsically

fluorescent carbon dots with tunable emission derived from hydrothermal treatment of glucose in the presence of monopotassium phosphate. Chem Commun 2011;47:11615–7. doi:10.1039/c1cc14860e.

[46] Oza G, Oza K, Pandey S, Shinde S, Mewada A, Thakur M, et al. A green route towards highly photoluminescent and cytocompatible carbon dot synthesis and its separation using sucrose density gradient centrifugation. J Fluoresc 2015;25:9–14. doi:10.1007/s10895-014-1477-x.

[47] Thakur M, Pandey S, Mewada A, Patil V, Khade M, Goshi E, et al. Antibiotic Conjugated Fluorescent Carbon Dots as a Theranostic Agent for Controlled Drug Release, Bioimaging, and Enhanced Antimicrobial Activity. J Drug Deliv 2014;2014:1–9. doi:10.1155/2014/282193.

[48] Pandey S, Mewada A, Oza G, Thakur M, Mishra N, Sharon M, et al. Synthesis and centrifugal separation of fluorescent carbon dots at room temperature. Nanosci Nanotechnol Lett 2013;5:775–9.

[49] Gaborieau M, Castignolles P. Size-exclusion chromatography (SEC) of branched polymers and polysaccharides. Anal Bioanal Chem 2011;399:1413–23. doi:10.1007/s00216-010-4221-7.

[50] Hong P, Koza S, Bouvier ES. A review size-exclusion chromatography for the analysis of protein biotherapeutics and their aggregates. J Liq Chromatogr Relat Technol 2012;35:2923–50.

[51] Kokorina AA, Prikhozhdenko ES, Tarakina N V., Sapelkin A V., Sukhorukov GB, Goryacheva IY. Dispersion of optical and structural properties in gel column separated carbon nanoparticles. Carbon N Y 2018;127:541–7. doi:10.1016/j.carbon.2017.11.039.

[52] Anilkumar P, Wang X, Cao L, Sahu S, Liu JH, Wang P, et al. Toward quantitatively fluorescent carbon-based "quantum" dots. Nanoscale 2011;3:2023–7. doi:10.1039/c0nr00962h.

[53] Wang X, Cao L, Yang ST, Lu F, Meziani MJ, Tian L, et al. Bandgap-like strong fluorescence in functionalized carbon nanoparticles. Angew Chemie - Int Ed 2010;49:5310–4. doi:10.1002/anie.201000982.

[54] Arcudi F, Dordevic L, Prato M. Synthesis, separation, and characterization of small and highly fluorescent nitrogen-doped carbon nanodots. Angew Chemie - Int Ed 2016;55:2107–12. doi:10.1002/anie.201510158.

[55] Wang Q, Zhang S, Zhong Y, Yang XF, Li Z, Li H. Preparation of Yellow-Green-Emissive Carbon Dots and Their Application in Constructing a Fluorescent Turn-On

Nanoprobe for Imaging of Selenol in Living Cells. Anal Chem 2017;89:1734–41. doi:10.1021/acs.analchem.6b03983.

[56] Vinci JC, Colon LA. Fractionation of carbon-based nanomaterials by anion-exchange HPLC. Anal Chem 2012;84:1178–83. doi:10.1021/ac202667x.

[57] Vinci JC, Ferrer IM, Seedhouse SJ, Bourdon AK, Reynard JM, Foster BA, et al. Hidden properties of carbon dots revealed after HPLC fractionation. J Phys Chem Lett 2013;4:239–43. doi:10.1021/jz301911y.

[58] Ding H, Yu SB, Wei JS, Xiong HM. Full-color light-emitting carbon dots with a surface-state-controlled luminescence mechanism. ACS Nano 2016;10:484–91. doi:10.1021/acsnano.5b05406.

[59] Gong X, Hu Q, Paau MC, Zhang Y, Shuang S, Dong C, et al. Red-green-blue fluorescent hollow carbon nanoparticles isolated from chromatographic fractions for cellular imaging. Nanoscale 2014;6:8162–70. doi:10.1039/c4nr01453g.

[60] Gong X, Hu Q, Chin Paau M, Zhang Y, Zhang L, Shuang S, et al. High-performance liquid chromatographic and mass spectrometric analysis of fluorescent carbon nanodots. Talanta 2014;129:529–38. doi:10.1016/j.talanta.2014.04.008.

[61] Hu Q, Paau MC, Choi MMF, Zhang Y, Gong X, Zhang L, et al. Better understanding of carbon nanoparticles via high-performance liquid chromatography-fluorescence detection and mass spectrometry. Electrophoresis 2014;35:2454–62. doi:10.1002/elps.201400197.

[62] Zhou Y, Liyanage PY, Geleroff DL, Peng Z, Mintz KJ, Hettiarachchi SD, et al. Photoluminescent Carbon Dots: A Mixture of Heterogeneous Fractions. ChemPhysChem 2018;19:2589–97. doi:10.1002/cphc.201800248.

[63] Xu X, Ray R, Gu Y, Ploehn HJ, Gearheart L, Raker K, et al. Electrophoretic analysis and purification of fluorescent single-walled carbon nanotube fragments. J Am Chem Soc 2004;126:12736–7. doi:10.1021/ja040082h.

[64] Ehrat F, Bhattacharyya S, Schneider J, Lo A, Wyrwich R, Rogach AL, et al. Tracking the Source of Carbon Dot Photoluminescence: Aromatic Domains versus Molecular Fluorophores 2017. doi:10.1021/acs.nanolett.7b03863.

[65] Kokorina AA, Bakal AA, Beloglazova N V., De Saeger S, Sukhorukov GB, Sapelkin A V., et al. Separation of citric acid-ethylenediamine derived carbon nanodots by gel electrophoresis: impact of size and charge dispersion on the light emission. NanoLetters 2019;2:25.

[66] Hu Q, Paau MC, Zhang Y, Chan W, Gong X, Zhang L, et al. Capillary electrophoretic

study of amine/carboxylic acid-functionalized carbon nanodots. J Chromatogr A 2013;1304:234–40. doi:10.1016/j.chroma.2013.07.035.

[67] Dimaki M, Bøggild P. Dielectrophoresis of carbon nanotubes using microelectrodes : a numerical study 2004;1095. doi:10.1088/0957-4484/15/8/039.

Conflict of Interest and Authorship Conformation Form

- All authors have participated in (a) conception and design, or analysis and interpretation of the data; (b) drafting the article or revising it critically for important intellectual content; and (c) approval of the final version.

  All authors have participated in conception, design, analysis and interpretation of the data.

  All authors have participated in drafting the article or revising it critically for important intellectual content.

  All authors approved of the final version.

- This manuscript has not been submitted to, nor is under review at, another journal or other publishing venue.

  The manuscript **"Luminescent carbon nanoparticles separation and purification"** has not been submitted to another journal or other publishing venue.

- The authors have no affiliation with any organization with a direct or indirect financial interest in the subject matter discussed in the manuscript

- The following authors have affiliations with organizations with direct or indirect financial interest in the subject matter discussed in the manuscript:

Author's name	Affiliation

Luminescent carbon nanoparticles separation and purification

Commonly used centrifugation, dialysis or filtration techniques are necessary for removing large soot pieces or low molecular weight substances.

An addition of techniques for fine separation (sucrose density centrifugation, gel electrophoresis, chromatography) is based on various CNPs properties, such as density, properties (charge, hydrophobicity) will allow not only to isolate CNPs fraction with uniform properties but charge, mass, size, hydrophobic or hydrophilic nature.

In the case of sucrose gradient centrifugation method, the smaller size nanoparticles collected in a layer with a larger density compare to the larger ones, which is indicated by their penetration to the sucrose layers with larger density.

The size-exclusion chromatography provides an effective tool for extracting fractions with different properties (optical and/or size) that is essential for consequent comparative analysis.

The selection of gel electrophoresis experimental parameters such as buffer solution, pH, amperage, gel nature, and concentration allows effective sample separation. Furthermore, the possibility of a combination of gel electrophoresis and optical detections methods can provide detailed information about the nature and origin of light emission in CNPs.